A Dansyl Amide *N*-Oxide Fluorogenic Probe Based on a Bioorthogonal Decaging Reaction

Hong Yang, Yongcheng Wang, Xiang Li, Yu Teng, and Yulin Tian*[a]

A smart fluorescence "turn-on" probe which contained a dansyl amide fluorophore and an *N*-oxide group was designed based on the bioorthogonal decaging reaction between *N*-oxide and the boron reagent. The reaction proceeds in a rapid kinetics ($k_2 = 57.1 \pm 2.5\ M^{-1}s^{-1}$), and the resulting reduction product showcases prominent fluorescence enhancement (up to 72-fold). Time dependent density functional theoretical (TD-DFT) calculation revealed that the process of photoinduced electron transfer (PET) from the *N*-oxide moiety to the dansyl amide fluorophore accounts for the quenching mechanism of *N*-oxide. This probe also showed high selectivity over various nucleophilic amino acids and good biocompatibility in physiological conditions. The successful application of the probe in HaloTag protein labeling and HepG2 live-cell imaging proves it a valuable tool for visualization of biomolecules.

1. Introduction

Bioorthogonal reaction-based fluorescent turn-on probes are remarkable chemical tools to label and image biological macromolecules such as glycans, lipids, nucleic acids, and proteins in biological systems.[1] They are typically designed based on profluorophores bearing a bifunctional group, which is a fluorescence quencher as well as a bioorthogonal handle. Upon a bioorthogonal reaction, a new chemical functionality is generated and high fluorescence enhancement is achieved by converting profluorophore to fluorophore.[2] Compared to the conventional "Always-ON'' type fluorophores, these OFF-ON type probes have higher signal-to-noise ratio, better contrast of images and better chance to avoid washing steps, offering valuable tools for live cell imaging[3] In the past few years, several powerful fluorogenic probes have been developed, which employ a series of bioorthogonal groups such as azido,[4] alkyne,[5] sydnone,[6,7] oxime,[8] hydrazine,[9] or tetrazine[10] to quench fluorophores, and the fluorescence was usually restored after bioorthogonal bond-formation reactions.

Recently, photo-induced and chemical-induced bioorthogonal decaging reactions have attracted great attention.[11–13] These reactions provided important tools to study and manipulate biomolecules in a highly spatiotemporally controlled manner in physiological systems ranging from proteins to intact cells.[14] A series of decaging-based fluorogenic probes have also been widely used for bioimaging, such as allylic/propargyl/vinyl-modified coumarin,[15,16] fluorescein,[17,18] rhodamine,[19,20] and cyanine[21] dyes. The bioorthogonal decaging reaction of *N*-oxide and boron reagents has been identified as a rapid, sensitive, benign toxic and inherent biocompatible reaction, thus was well-suited for activating molecules within cells under chemical control.[22] Here, an *N*-oxide modified dansyl amide-based fluorogenic probe (DASNox) was designed and synthesized, which showed significant fluorescence enhancement after treatment with the boron reagent. We evaluated its photophysical properties, reaction kinetics and biocompatibility, and employed the probe for protein labeling and cell imaging.

2. Results and Discussion

2.1. Design, Synthesis and Photophysical Properties of DASNox

As a typical internal charge transfer (ICT)-based fluorophore, dansyl amide contains both electron-donating group (dimethylamino group at 5-position) and electron-withdrawing group (sulfonyl group at 1-position), composing a "push–pull"-electron system, which exhibits high fluorescence quantum yield, good photostability, and large stokes shift.[23] For the molecular probe design, the electron-withdrawing *N*-oxide group was introduced at the 5-position of dansyl amide, creating a "pull–pull" system that block the ICT process to achieve the dark "turn-off" state, while a polyethylene glycol-type hydrophilic chain was attached to the sulfonamide for increasing the probe's water solubility (DASNox, Figure 1a).

DASNox can be easily prepared by the oxidation of corresponding parent fluorophore dansyl amide (DAS) in the presence of meta-chloroperoxybenzoic acid (mCPBA) in ethyl acetate (Figure 1a). Next, photophysical properties of DASNox were determined in mixture solvent (acetonitrile/PBS = 2:1, v/v) and compared with that of DAS (Table 1, Figure 1b, and

[a] Dr. H. Yang, Dr. Y. Wang, X. Li, Y. Teng, Dr. Y. Tian
Key Laboratory of Bioactive Substances and Function of Natural Medicine
Beijing Key Laboratory of Active Substances Discovery and Drugability Evaluation
Institute of Materia Medica
Peking Union Medical College and Chinese Academy of Medical Sciences
1 Xian Nong Tan Street, 100050 Beijing (China)
E-mail: tianyulin@imm.ac.cn

Supporting information for this article is available on the WWW under https://doi.org/10.1002/open.202100104

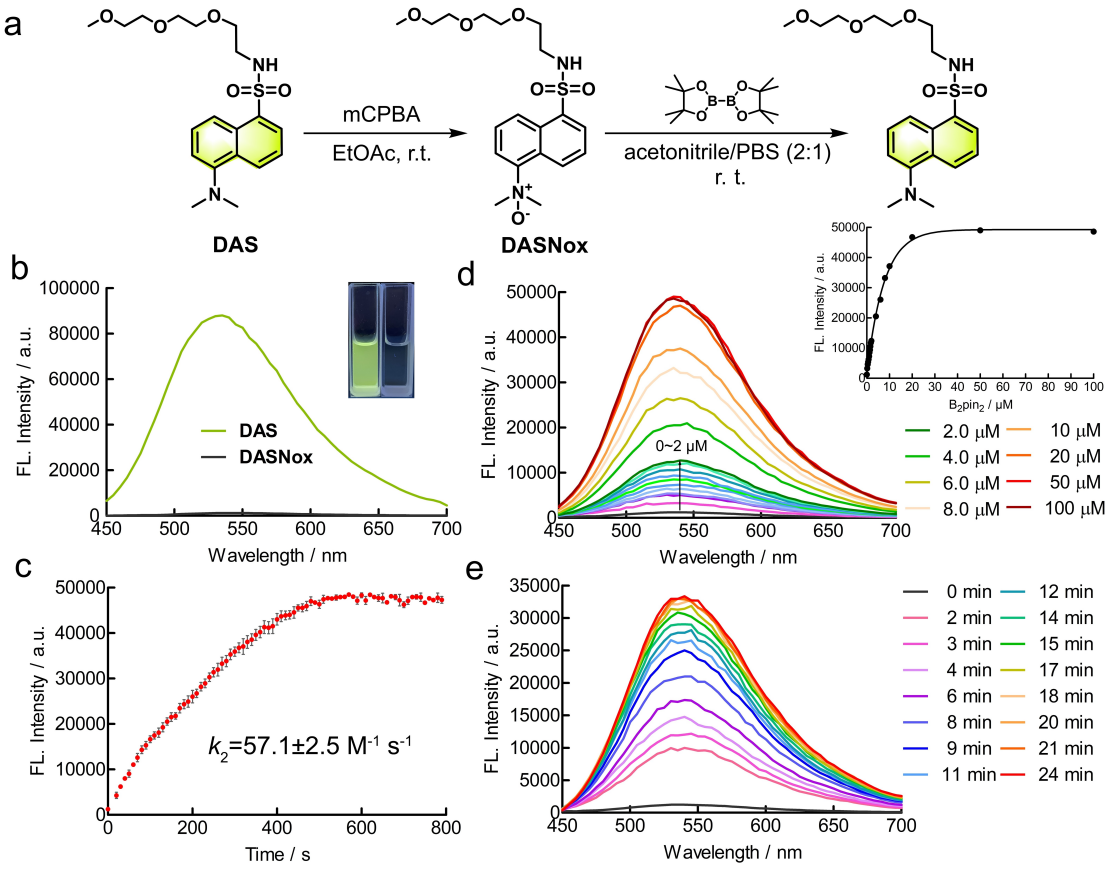

Figure 1. (a) Synthesis of DASNox and the bioorthogonal decaging turn-on reaction between DASNox and B_2pin_2. (b) Fluorescence emission spectra of 10 μM DASNox and DAS in acetonitrile/PBS (2:1, v/v). (c) Reaction kinetics of 10 μM DASNox with 100 μM B_2pin_2 in acetonitrile/PBS (2:1, v/v). (d) Fluorescence emission spectra of 10 μM DASNox after reaction with 0~100 μM B_2pin_2 in acetonitrile/PBS (2:1, v/v) for 10 min. (e) Fluorescence emission spectra of 10 μM DASNox after reaction with 10 μM B_2pin_2 for 0~24 min in acetonitrile/PBS (2:1, v/v).

Table 1. Photophysical properties of DASNox and DAS in mixture solvent (acetonitrile/PBS = 2:1, v/v).[a]

Probe	λ_{abs} [nm]	λ_{em} [nm][b]	Stokes Shift [nm]	ε [M^{-1}cm^{-1}]	Φ[c]	Turn-on[d]
DASNox	320	535	215	412	0.01	–
DAS	338	535	197	4186	0.22	72

[a] All test samples were prepared at the concentration of 10 μM in acetonitrile/PBS (2:1, v/v). [b] Determined at λ_{exc} = 340 nm. [c] Fluorescence quantum yield, quinine sulfate in aqueous 0.1 N H_2SO_4 as standard. [d] Fluorescence turn-on ratio of DAS towards DASNox.

Figure S1 in the Supporting Information). As we predicted, the *N*-oxide significantly quenched the dansyl amide dye, with DASNox exhibiting very low fluorescence quantum yield (Φ_F = 0.01) compared to fluorescent DAS (Φ_F = 0.22) (Figure 1b). In addition, the much lower molar absorption of DASNox (412 M^{-1}cm^{-1}) compared to that of DAS (4186 M^{-1}cm^{-1}) indicated the isolation of *N*-oxide from π-conjugation of the fluorophore.

Next, bioorthogonal decaging turn-on reaction was conducted by treating DASNox with a typical boron reagent, bis(pinacolato)diboron (B_2pin_2)[24] (Figure 1a). Boron-containing compounds have been generally considered to be low toxic to biological systems[25] and have been incorporated into chemical biology methods, such as in boronic acid-based sensors[26] and fluorescent probes.[27] As expected, the addition of B_2pin_2 induced a significant fluorescence enhancement, indicating that the deoxygenation of *N*-oxide successfully rebuilds the "push-pull" system and restores the ICT process (Figure 1d and 1e). The fluorescence intensity of the probe increased linearly with the increment of B_2pin_2 concentration in the range of 0~2 μM B_2pin_2, and reached maximum value in case of 20 μM B_2pin_2 in 10 min (Figure 1d). Besides, the fluorescence enhancement was recorded in a perceptible time-dependent manner (Figure 1e). On this basis, the reaction kinetics was evaluated by fluorescence measurement using 10 μM DASNox and 100 μM B_2pin_2, giving the second order rate constant of 57.1 ± 2.5 M^{-1}s^{-1} (Figure 1c), which is comparable to other bioorthogonal decaging reactions.[28]

2.2. Fluorescence Quenching Mechanism of DASNox

To elucidate the influence of *N*-oxide group on photophysical properties of DASNox and gain insights into the fluorescent differences between DASNox and DAS, TD-DFT calculations were performed at B3LYP/6-311+G(d) level using a polarized continuum model (PCM) in acetonitrile solvent. The optimized geometries, the highest occupied molecular orbitals (HOMO) and the lowest unoccupied molecular orbitals (LUMO) of simplified model probes DAS-1 and DASNox-1 are shown in Figure 2 and Table S1–2 in the Supporting Information. TD-DFT calculation revealed that the fluorescent emission of two molecules comes from the $S_1 \rightarrow S_0$ transition. For DASNox-1, the calculated oscillator strength (f) is only 0.0024, which confirmed its non-radiative character and dark state. In contrast, DAS-1 exhibited an allowed $S_1 \rightarrow S_0$ transition (f = 0.1428), hinting the presence of an emissive S_1 state and the fluorescence feature of DAS probe (Table S3 in the Supporting Information).

Next, we interpreted the fluorescence quenching mechanism by frontier molecular orbital (FMO) analysis. The optimized geometry of DASNox-1 revealed a nonplanar connection between oxygen atom of *N*-oxide and dansyl amide with a dihedral angle of 48.5°, implying a separation of donor and acceptor units due to their nearly orthogonal disposition in space (Figure 2a). As a result, the dansyl amide unit serves as a free fluorophore and the oxygen moiety refers to a free donor. LUMO of DASNox-1 was mainly distributed on naphthalene scaffold (fluorophore), while HOMO was restricted on *N*-oxide moiety (donor). PET from the *N*-oxide moiety to the dansyl amide fluorophore was evoked since the HOMO energy of the fluorophore (−6.79 eV, i.e. the HOMO-2 of the whole molecule DASNox-1) is lower than that of the donor (−5.99 eV, i.e. the HOMO of the whole molecule DASNox-1), which results in fluorescence quenching (Figure 2b). For DAS-1, HOMO was distributed on dansyl amide, while LUMO was mainly localized on naphthalene scaffold. Electron excitation from HOMO to LUMO could make the electronic density flow primarily from 5-position dimethylamine to naphthalene moiety, suggesting that the PET quenching process was blocked and strong fluorescence was produced.

2.3. Biocompatibility of DASNox

To ascertain the toxicity of DASNox and B_2pin_2 to cells, we subjected the HepG2 cells to the MTT cell viability assay (Figure S2 in the Supporting Information). The results indicated that both DASNox and B_2pin_2 showed negligible toxicity against HepG2 cells at least at the concentrations $< 100\ \mu M$, demonstrating the biocompatibility of thisbioorthogonal pair. Furtherly, we evaluated the influence of various amino acids on probe's fluorescence intensity change. As a result, DASNox showed prominent fluorescence response to B_2pin_2 compared to nucleophilic amino acids (Met, Cys, Glu, Asp, His, Lys, Arg, Thr) which couldn't trigger significant increase in fluorescence (Figure 3a), implying probe's high selectivity for B_2pin_2. Furthermore, we tested the stability of DASNox in cell lysates. The results showed that it didn't exhibit obvious fluorescence enhancement in HepG2 lysates in the absence of B_2pin_2 over 24 hours, demonstrating a good stability in physiological conditions (Figure 3b).

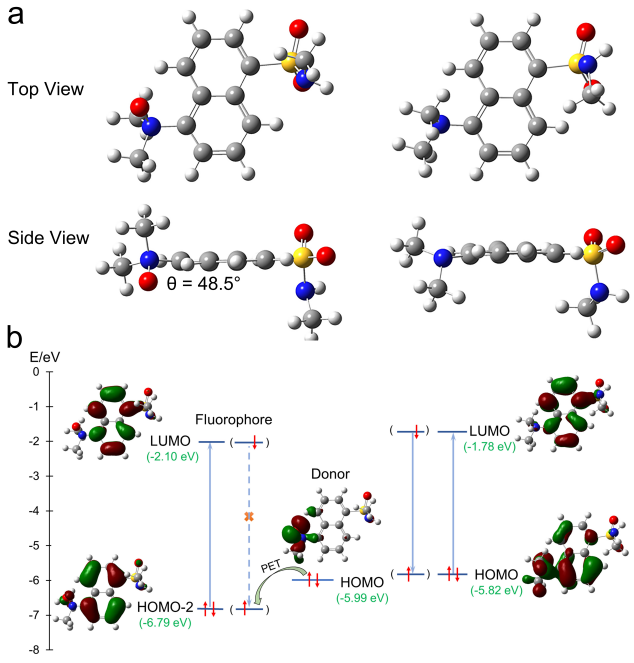

Figure 2. (a) Optimized geometries for DASNox-1 (left) and DAS-1 (right) in top and side view. (b) Energy levels of the frontier molecular orbitals of two probes and illustration of the PET process for DASNox-1.

2.4. Protein Labeling

Furthermore, we applied this decaging turn-on reaction to protein labeling using HaloTag technology, a typical method for incorporating functional small molecules into proteins of interest.[29] A dansyl amide *N*-oxide bearing HaloTag chloroalkane ligand, DASNoxHAL, was designed and synthesized, which was subsequently conjugated to the expressed 33 kDa HaloTag protein to produce DASNox-modified protein, HaloTag–DASNox (Figure 4a). After purification by size-exclusion chromatography,

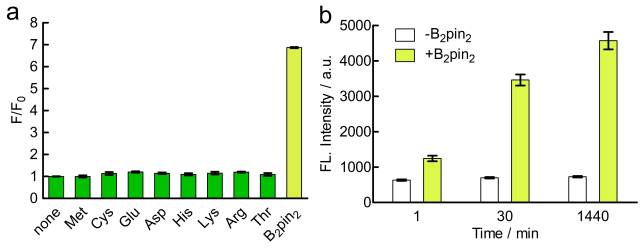

Figure 3. (a) Fluorescence intensity of 2 μM DASNox after incubated with 20 μM various amino acids in acetonitrile/PBS (2:1, v/v) for 1 h. (b) Fluorescence intensity of 2 μM DASNox in the presence and absence of B_2pin_2 in HepG2 cell lysates from 1 min to 24 h.

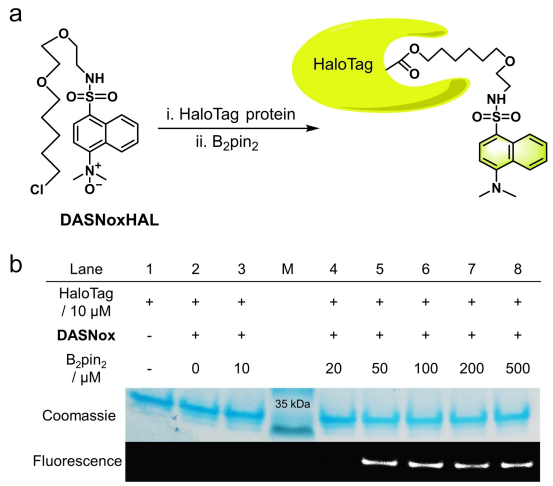

Figure 4. (a) DASNoxHAL was conjugated to HaloTag protein, then activated with B_2pin_2. (b) In gel visualization of the labeling of HaloTag-DASNox (10 μM) by treated with 0~50 equivalent B_2pin_2 for 5 min.

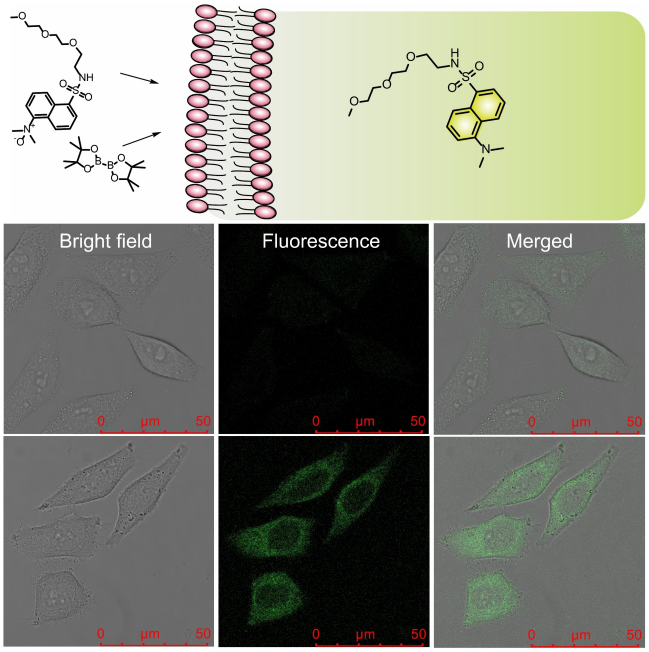

Figure 5. The in-cell decaging turn-on reaction. HepG2 cells were incubated with 5 μM DASNox for 30 min, washed, then incubated with buffer (up) or 100 μM B_2pin_2 (down) for 45 min. Pictures were taken using a confocal microscope.

10 μM HaloTag–DASNox was treated with 0, 10, 20, 50, 100, 200, 500 μM B_2pin_2 for 5 min, then analyzed by SDS-PAGE and in-gel fluorescence imaging. Figure 4b shows that 5 equivalents of B_2pin_2 are adequate to fully activate the fluorophore in 5 min. As control, no fluorescent band for HaloTag–DASNox was observed in absence of B_2pin_2, verifying the specificity of the reaction. The results have validated the robustness and chemical controllability of this decaging turn-on reaction for in situ fluorogenic protein labeling.

2.5. Cell Imaging

Finally, the in-cell fluorogenic reaction between DASNox and B_2pin_2 was investigated using HepG2 cells. Upon incubation with 5 μM DASNox for 30 min, the cells were washed and treated with 100 μM B_2pin_2 for 45 min, then directly submitted to confocal microscopy imaging without further washing steps. As a consequence, a clear appearance of the characteristic fluorescence of the corresponding DAS product was observed. As comparison, the control cells without B_2pin_2 treatment showed rather weak fluorescence (Figure 5 and S3 in the Supporting Information). These results demonstrated the cell-permeability of DASNox and illustrated the excellent applicability of this bioorthogonal system in the complex biological context.

3. Conclusion

In conclusion, we have developed dansyl amide *N*-oxide (DASNox) as a novel fluorogenic probe based on reduction-triggered decaging reaction. The probe reacts with B_2pin_2 in a rapid kinetics ($57.1 \pm 2.5\ M^{-1}s^{-1}$) to afford deoxidation product, which exhibits notable fluorescence enhancement (up to 72-fold). DFT calculations revealed that PET process from the *N*-oxide moiety to the dansyl amide fluorophore accounts for the fluorescence quenching mechanism of DASNox. Moreover, this probe proves stable in physiological conditions and showcases good compatibility over various biological analytes, which has been successfully applied in chemically controlled in situ proteins labeling and mammalian live-cell imaging. However, its relatively low fluorescence intensity in aqueous biosystem and UV excitationwavelength range may restrict its applications in living organism labeling. This bioorthogonal decaging-based turn-on methodology has enriched the chemical biology toolkit and offered an effective way for visualization and detection of biomolecules in vivo.

Experimental Section

Materials and Instruments

Solvents and chemicals were purchased from commercial sources and used directly without further purification. Fast-*pfu* DNA polymerase, Seamless Cloning and assembly kit, and restriction enzymes were purchased from TransGen (Beijing, China). ^{1}H NMR spectra were recorded on a Varian 400 MHz NMR spectrometer. ^{13}C NMR spectra were recorded on a Varian 400 MHz NMR spectrometer. ESI-HRMS data were measured on Thermo LCQ Deca XP Max mass spectrometer. Silica gel flash column chromatography was performed on Biotage Isolera one. Fluorescence emission spectra and full wavelength absorption spectra were recorded on Tecan Spark™ 10 M Multimode Microplate Reader. Confocal fluorescence images were acquired with Leica TCS SP8 X Confocal Microscope.

Synthesis Procedures and Characterization Data

5-(dimethylamino)-*N*-(2-(2-(2-methoxyethoxy)ethoxy)ethyl) naphthalene-1-sulfonamide (DAS). To a solution of 5-(dimethylamino)naphthalene-1-sulfonyl chloride (150 mg, 0.56 mmol) in DCM (5 mL) was added Et_3N (68 mg, 0.67 mmol) and 2-(2-(2-methoxyethoxy)ethoxy)ethanamine (99 mg, 0.61 mmol). The mixture was stirred at room temperature for 2 h, then concentrated. The residue was purified by silica gel flash column chromatography (PE/EtOAc = 2:1) to afford the titled compound as yellow oil (206 mg, 93% yield). ^{1}H NMR (400 MHz, $CDCl_3$) δ 8.54 (d, J = 8.5 Hz, 1H), 8.32 (d, J = 8.6 Hz, 1H), 8.23 (d, J = 8.4 Hz, 1H), 7.60–7.47 (m, 2H), 7.19 (d, J = 7.5 Hz, 1H), 5.55 (t, J = 5.9 Hz, 1H), 3.60–3.56 (m, 2H), 3.55–3.51 (m, 2H), 3.50–3.45 (m, 2H), 3.40–3.33 (m, 7H), 3.13–3.07 (m, 2H), 2.89 (s, 6H); ^{13}C NMR (100 MHz, $CDCl_3$) δ 151.73, 135.24, 130.28, 129.85, 129.71, 129.35, 128.28, 123.31, 119.21, 115.29, 71.91, 70.49, 70.30, 70.23, 69.25, 59.06, 45.50, 43.10; HRMS (ESI) calcd for $C_{19}H_{29}N_2O_5S$ 397.1792 [M + H$^+$], found 397.1793.

5-(*N*-(2-(2-(2-methoxyethoxy)ethoxy)ethyl)sulfamoyl)-*N*,*N*-dimethyl naphthalen-1-amine oxide (DASNox). To a solution of DAS (40 mg, 0.1 mmol) in EtOAc (2 mL) was added *m*-CPBA (26 mg, 0.15 mmol). The mixture was stirred at room temperature for 6 h, then concentrated. The residue was purified by silica gel flash column chromatography (DCM/MeOH = 7:1) to afford the titled compound as colorless oil (32 mg, 76% yield). ^{1}H NMR (400 MHz, CD_3OD) δ 9.39 (d, J = 8.9 Hz, 1H), 8.96 (d, J = 8.7 Hz, 1H), 8.35 (d, J = 6.8 Hz, 1H), 8.11 (d, J = 7.9 Hz, 1H), 7.82–7.67 (m, 2H), 4.03 (s, 6H), 3.58–3.54 (m, 2H), 3.53–3.48 (m, 2H), 3.47–3.43 (m, 2H), 3.38–3.32 (m, 7H), 3.09 (t, J = 5.4 Hz, 2H);^{13}C NMR (100 MHz, CD_3OD) δ 145.19, 137.67, 130.63, 129.95, 129.18, 128.67, 126.15, 125.81, 125.56, 118.94, 71.41, 69.90, 69.83, 69.62, 69.18, 60.62, 57.66, 42.45; HRMS (ESI) calcd for $C_{19}H_{29}N_2O_6S$ 413.1741 [M + H$^+$], found 413.1745.

***N*-(2-(2-((6-chlorohexyl)oxy)ethoxy)ethyl)-5-(dimethyl amino) naphthalene-1-sulfonamide (DASHAL)**. To a solution of 5-(dimethylamino)naphthalene-1-sulfonyl chloride (270 mg, 1.00 mmol) in DCM (10 mL) was added Et_3N (152 mg, 1.50 mmol) and 2-(2-((6-chlorohexyl)oxy)ethoxy)ethan-1-amine[30] (223 mg, 1.00 mmol). The mixture was stirred at room temperature for 2 h, then concentrated. The residue was purified by silica gel flash column chromatography (PE/EtOAc = 2:1) to afford the titled compound as light yellow oil (280 mg, 61% yield). ^{1}H NMR (400 MHz, $CDCl_3$) δ 8.54 (d, J = 8.4 Hz, 1H), 8.30 (d, J = 8.8 Hz, 1H), 8.24 (dd, J = 7.2, 1.2 Hz, 1H), 7.60–7.48 (m, 2H), 7.19 (d, J = 7.6 Hz, 1H), 5.34 (t, J = 6.0 Hz, 1H), 3.52 (t, J = 6.8 Hz, 2H), 3.45–3.31 (m, 8H), 3.16–3.05 (m, 2H), 2.89 (s, 6H), 1.83–1.70 (m, 2H), 1.62–1.55 (m, 2H), 1.48–1.40 (m, 2H), 1.40–1.32 (m, 2H); ^{13}C NMR (100 MHz, $CDCl_3$) δ 152.06, 135.17, 130.48, 130.03, 129.79, 129.48, 128.39, 123.30, 119.04, 115.30, 71.40, 70.44, 69.95, 69.32, 45.54, 45.18, 43.21, 32.61, 29.49, 26.77, 25.51; HRMS (ESI) calcd for $C_{22}H_{34}N_2O_4ClS$ 457.1922 [M + H$^+$], found 457.1943.

5-(*N*-(2-(2-((6-chlorohexyl)oxy)ethoxy)ethyl)sulfamoyl)-*N*,*N*-dimethylnaphthalen-1-amine oxide (DASNoxHAL). To a solution of DASHAL (260 mg, 0.57 mmol) in EtOAc (5 mL) was added *m*-CPBA (118 mg, 0.68 mmol), the mixture was stirred at room temperature for 6 h, then concentrated. The residue was purified by silica gel flash column chromatography (DCM/MeOH = 10:1) to afford the titled compound as colourless oil (160 mg, 59% yield). ^{1}H NMR (400 MHz, $CDCl_3$) δ 10.10–9.86 (m, 1H), 8.84 (d, J = 8.8 Hz, 1H), 8.34–8.24 (m, 1H), 7.93 (t, J = 7.6 Hz, 1H), 7.68–7.49 (m, 2H), 3.91 (s, 6H), 3.54–3.41 (m, 10H), 3.13–3.03 (m, 2H), 1.82–1.70 (m, 2H), 1.66–1.53 (m, 2H), 1.50–1.30 (m, 4H).; ^{13}C NMR (100 MHz, $CDCl_3$) δ 149.02, 136.43, 132.20, 131.01, 129.66, 129.58, 127.49, 126.11, 125.05, 117.49, 71.42, 70.44, 70.03, 69.58, 63.02, 45.20, 43.10, 32.61, 29.51, 26.78, 25.52; HRMS (ESI) calcd for $C_{22}H_{34}N_2O_5ClS$ 473.1871 [M + H$^+$], found 473.1879.

Kinetics Measurement

The bioorthogonal cleavage reaction kinetics measurements were performed at room temperature in TECAN fluorescence plate reader equipped with automatic injection unit. Two μL of 1 mM DASNox in DMSO was pipetted into each well containing 178 μL acetonitrile/PBS (2:1). To this solution was added 20 μL of 1 mM B_2pin_2 in acetonitrile/PBS (2:1). The final concentration of DASNOX was 10 μM, and the final concentration of B_2pin_2 was 100 μM. The well plate was inserted into plate reader and the measurement was immediately started. The excitation wavelength was set to 340 nm and the fluorescence intensities were collected at 535 nm every 10 s. Plots of fluorescence intensity vs. reaction time were recorded and the amounts of cleavage product were fitted to an exponential rise to maximum equation, $y = (y^0 - a)\, e^{kt} + a$, to give k. The second-order rate constant, k_2, were calculated using the following equation: $k_2 = k/[B_2pin_2]$. Measurements were repeated three times at each time point to derive the mean and standard deviation.

DFT Calculations

All quantum chemical studies were performed with the Gaussian 09 software.[31] Molecular structures for DAS-1 and DASNox-1 were obtained by optimizing their geometries at the DFT-B3LYP level with 6-311G(d) basis set using IEFPCM model to include solvent (CH_3CN) effect. Oscillator strengths (f) were computed based on the solvent-equilibrated ground-state geometries using time-dependent DFT (TD-DFT) with the 6-311 + G(d) basis set with added diffuse functions. Electron density differences between the ground and respective excited states were determined from the corresponding Gaussian cube output files.

Plasmid Construction

Construct plasmid pET28b(+)-HaloTag: The HaloTag gene was PCR amplified from pHTC-HaloTag with primers HaloTag-F:CTTTAA-AGAAGGAGATATACCATGCAGAA ATCGGTACTGG and HaloTag-R: TCAGTGGTGGTGGTGGTGGTGCTC and gel purified. Plasmid pET28b (+) (Novagen) was linearized by restriction site digestion with *Nco*I and *Xho*I (1 h, 37 °C) then gel purified. The vector (100 ng) was combined with the HaloTag PCR product in a 1:2 molar ratio and assembled by assembly kit. The assembly mixture (5 μL) was transformed into chemically competent *E. coli Trans*1-T1 (TransGen, Beijing, China) cells and selected on kanamycin LB/agar plates. Several of the resulting colonies were selected and used to inoculate 5 mL of LB media with 50 μg/mL kanamycin. Plasmids were isolated using a miniprep kit and sequence verified.

HaloTag Protein Purification

The recombinant plasmid pET28b(+)-HaloTag (20 ng) was transformed into *E. coli* BL21 cells and selected on kanamycin LB/agar plates. A single colony was selected and used to inoculate LB media (50 mL) containing 50 μg/mL kanamycin. The starter culture was grown to saturation overnight. 1 L LB broth each containing 50 μg/mL kanamycin were inoculated by adding 10 mL starter culture and grown to OD ~0.8. Protein expression was induced with 1 mM IPTG at 18 °C overnight. The cells were pelleted by centrifugation (20 min, 5000 × g), and the supernatant was discarded. 20 mL buffer A (pH 7.6, 20 mM imidazole, 50 mM PBS, and 1 mg/mL Roche complete protease inhibitor) was added to the cell pellet and then disrupted by sonication (400 W, 40% amplitude) for 5 min, then centrifuged (4 °C, 12000 rpm) for 10 min. The supernatant was loaded onto a column containing Ni-NTA resin (1 mL, Qiagen) pre-equilibrated with buffer A. The column was washed with buffer A

containing 20, 40, 60, 80, 100 and 150 mM imidazole (10 mL) successively. The His-tagged HaloTag protein was eluted at buffer A containing 60 mM imidazole and concentrated to ~2 mL with an Amicon ultrafiltration centrifuge tube (10 kDa cutoff). The imidazole buffer was exchanged by four successive additions of 10 mM PBS containing 1 mg/mL protease inhibitor to $<20\,\mu M$ imidazole remaining, followed by concentration to ~2 mL with the centrifuge tube. The protein was then purified by size exclusion column chromatography (HiLoad 16/60 Superdex 75, GE Healthcare) on an FPLC with 10 mM PBS containing 1 mg/mL protease inhibitor. Pure fractions were collected and concentrated with a 10 kDa molecular weight cutoff filter. The protein concentration was determined to ~5.5 mg/mL (150 μM) by A280 measurements on Nanodrop (Thermo).

Preparation of HaloTag–DASNox

333 μL purified HaloTag protein solution (150 μM, 1 equiv) was reacted with 10 μL DASNoxHAL (10 mM, 2 equiv) at room temperature. After 1 h, the solution was concentrated to a volume of 250 μL with a 10 kDa molecular weight cutoff filter (Amicon). The conjugated protein was purified by size exclusion chromatography (HiLoad 16/60 Superdex 75, GE Healthcare) on an FPLC with 10 mM PBS containing 1 mg/mL protease inhibitor. Column fractions containing the protein were concentrated to a concentration of ~3.7 mg/mL (112 μM) with a 10 kDa molecular weight cutoff filter (Amicon).

In-Gel Fluorescence Labeling

A solution of HaloTag–DASNox (7.5 μL, 10 μM) were incubated with a solution of B_2pin_2 (7.5 μL, 0, 10, 20 and 50 μM) for 5 min. Each reaction was quenched with 4×SDS sample loading buffer containing trimethylamine *N*-oxide (TMAO, 3 μL, 500 mM). Unmodified HaloTag protein was used as control. The protein samples were analysed by SDS-PAGE and visualized by in-gel fluorescence scanning on SAGE ChampChemi imager. The gel was then subjected to coomassie blue staining.

HepG2 cells culture experiments

Human hepatocellular carcinoma (HepG2) cells were cultured in DMEM (Dulbecco's modified Eagle's medium) (Corning) containing 10% fetal bovine serum (Invitrogen) and 1% penicillin–streptomycin (Corning). All cell lines were maintained at a humidified incubator with 5% CO_2 at 37 °C. The cells (3.0×10^5) were seeded on Advanced TC glass-bottomed dishes (CELLviewTM Cell Culture Dish, Greiner) two days before use.

Confocal Fluorescence Imaging Experiments

Confocal fluorescence images were acquired with Leica TCS SP8 X Confocal Microscope using 63× magnification. Images were obtained with appropriate filter as excitation = 405 nm, emission = 480 ~ 580 nm. For the imaging experiments, cells were treated with 5 μM DASNox in DMEM without phenol red and FBS at 37 °C for 30 min. After washing twice with PBS, the well was added 100 μM B_2pin_2 in DMEM without phenol red and FBS, incubated for 45 min, then directly submitted for imaging using the confocal microscope. The control cells were treated with 5 μM DASNox in the absence of B_2pin_2.

Acknowledgements

This work was supported by the Beijing Nova Program (Z201100006820049), National Natural Science Foundation of China (21907109).

Conflict of Interest

The authors declare no conflict of interest.

Keywords: bioorthogonal decaging reactions · *N*-oxide · fluorogenic probes · protein labeling · cell imaging

[1] C. l. L. Droumaguet, C. Wang, Q. Wang, *Chem. Soc. Rev.* **2010**, *39*, 1233–1239.
[2] P. Shieh, C. R. Bertozzi, *Org. Biomol. Chem.* **2014**, *12*, 9307–9320.
[3] A. Nadler, C. Schultz, *Angew. Chem. Int. Ed.* **2013**, *52*, 2408–2410; *Angew. Chem.* **2013**, *125*, 2466–2469.
[4] P. Shieh, V. T. Dien, B. J. Beahm, J. M. Castellano, T. Wyss-Coray, C. R. Bertozzi, *J. Am. Chem. Soc.* **2015**, *137*, 7145–7151.
[5] Z. Zhou, C. J. Fahrni, *J. Am. Chem. Soc.* **2004**, *126*, 8862–8863.
[6] C. Favre, F. Friscourt, *Org. Lett.* **2018**, *20*, 4213–4217.
[7] E. Decuypere, M. Riomet, A. Sallustrau, S. Bregant, R. Thai, G. Pieters, G. Clavier, D. Audisio, F. Taran, *Chem. Commun.* **2018**, *54*, 10758–10761.
[8] Y. Tian, X. Li, D. Yin, *Chem. Commun.* **2019**, *55*, 12865–12868.
[9] X. Li, Y. Wang, H. Yang, D. Yin, Y. Tian, *Eur. J. Org. Chem.* **2020**, *2020*, 4296–4300.
[10] H. Wu, N. K. Devaraj, *Acc. Chem. Res.* **2018**, *51*, 1249–1259.
[11] Y. Li, H. Fu, *ChemistryOpen* **2020**, *9*, 835–853.
[12] J. Li, P. R. Chen, *Nat. Chem. Biol.* **2016**, *12*, 129–137.
[13] X. Ji, Z. Pan, B. Yu, L. K. De La Cruz, Y. Zheng, B. Ke, B. Wang, *Chem. Soc. Rev.* **2019**, *48*, 1077–1094.
[14] J. Tu, M. Xu, R. M. Franzini, *ChemBioChem* **2019**, *20*, 1615–1627.
[15] X. Fan, Y. Ge, F. Lin, Y. Yang, G. Zhang, W. S. Ngai, Z. Lin, S. Zheng, J. Wang, J. Zhao, J. Li, P. R. Chen, *Angew. Chem. Int. Ed.* **2016**, *55*, 14046–14050; *Angew. Chem.* **2016**, *128*, 14252–14256.
[16] J. Wang, S. Zheng, Y. Liu, Z. Zhang, Z. Lin, J. Li, G. Zhang, X. Wang, J. Li, P. R. Chen, *J. Am. Chem. Soc.* **2016**, *138*, 15118–15121.
[17] A. L. Garner, F. Song, K. Koide, *J. Am. Chem. Soc.* **2009**, *131*, 5163–5171.
[18] M. Santra, S. K. Ko, I. Shin, K. H. Ahn, *Chem. Commun.* **2010**, *46*, 3964–3966.
[19] A. M. Perez-Lopez, B. Rubio-Ruiz, V. Sebastian, L. Hamilton, C. Adam, T. L. Bray, S. Irusta, P. M. Brennan, G. Lloyd-Jones, D. Sieger, J. Santamaria, A. Unciti-Broceta, *Angew. Chem. Int. Ed.* **2017**, *56*, 12548–12552; *Angew. Chem.* **2017**, *129*, 12722–12726.
[20] M. A. Miller, B. Askevold, H. Mikula, R. H. Kohler, D. Pirovich, R. Weissleder, *Nat. Commun.* **2017**, *8*, 15906.
[21] H. Wu, S. C. Alexander, S. Jin, N. K. Devaraj, *J. Am. Chem. Soc.* **2016**, *138*, 11429–11432.
[22] J. Kim, C. R. Bertozzi, *Angew. Chem. Int. Ed.* **2015**, *54*, 15777–15781; *Angew. Chem.* **2015**, *127*, 16003–16007.
[23] P. Wang, J. Wu, Y. An, Y. Liao, *Spectrochim. Acta. Mol. Biomol. Spectrosc.* **2019**, *220*, 117140.
[24] C. A. G. Carter, K. D. John, G. Mann, R. L. Martin, T. M. Cameron, R. T. Baker, K. L. Bishop, R. D. Broene, S. A. Westcottin, *Group 13 Chemistry: From Fundamentals to Applications* (Eds.: P. J. Shapiro, D. A. Atwood), ACS Publications, Washington, DC, **2002**, pp. 70–87.
[25] J. C. Carlson, H. Mikula, R. Weissleder, *J. Am. Chem. Soc.* **2018**, *140*, 3603–3612.
[26] E. C. Neeve, S. J. Geier, I. A. Mkhalid, S. A. Westcott, T. B. Marder, *Chem. Rev.* **2016**, *116*, 9091–9161.
[27] G. Fang, H. Wang, Z. Bian, J. Sun, A. Liu, H. Fang, B. Liu, Q. Yao, Z. Wu, *RSC Adv.* **2018**, *8*, 29400–29427.
[28] S. Xu, A. C. Sedgwick, S. A. Elfeky, W. Chen, A. S. Jones, G. T. Williams, A. T. A. Jenkins, S. D. Bull, J. S. Fossey, T. D. James, *Front. Chem.* **2020**, *14*, 112–116.
[29] C. G. England, H. Luo, W. Cai, *Bioconjugate Chem.* **2015**, *26*, 975–986.

[30] S. Rubner, A. Scharow, S. Schubert, T. Berg, *Angew. Chem.* **2018**, *130*, 17289–17293; *Angew. Chem. Int. Ed.* **2018**, *57*, 17043–17047.
[31] Gaussian 09, Revision E.01, M. J. Frisch, G. W. Trucks, H. B. Schlegel, G. E. Scuseria, M. A. Robb, J. R. Cheeseman, G. Scalmani, V. Barone, G. A. Petersson, H. Nakatsuji, X. Li, M. Caricato, A. Marenich, J. Bloino, B. G. Janesko, R. Gomperts, B. Mennucci, H. P. Hratchian, J. V. Ortiz, A. F. Izmaylov, J. L. Sonnenberg, D. Williams-Young, F. Ding, F. Lipparini, F. Egidi, J. Goings, B. Peng, A. Petrone, T. Henderson, D. Ranasinghe, V. G. Zakrzewski, J. Gao, N. Rega, G. Zheng, W. Liang, M. Hada, M. Ehara, K. Toyota, R. Fukuda, J. Hasegawa, M. Ishida, T. Nakajima, Y. Honda, O. Kitao, H. Nakai, T. Vreven, K. Throssell, J. A. Montgomery, Jr., J. E. Peralta, F. Ogliaro, M. Bearpark, J. J. Heyd, E. Brothers, K. N. Kudin, V. N. Staroverov, T. Keith, R. Kobayashi, J. Normand, K. Raghavachari, A. Rendell, J. C. Burant, S. S. Iyengar, J. Tomasi, M. Cossi, J. M. Millam, M. Klene, C. Adamo, R. Cammi, J. W. Ochterski, R. L. Martin, K. Morokuma, O. Farkas, J. B. Foresman„ D. J. Fox, Gaussian, Inc., Wallingford CT, **2009**.

Manuscript received: May 8, 2021
Revised manuscript received: September 10, 2021